STAG: Smart Tools and Apps in computer Graphics (2016)
Giovanni Pintore and Filippo Stanco (Editors)

Design and Fabrication of Grid-shells Mockups

Davide Tonelli[1],Nico Pietroni[2], Paolo Cignoni[1] and Roberto Scopigno[1]

[1] RFR Paris [2]ISTI, CNR, Italy

Abstract

Statics Aware Voronoi Grid-shells have been recently introduced in the Architectural Geometry field. These are innovative grid-shells endowed with a polygonal topology, whose geometry is structurally optimized by means of a novel algorithm [PTP+15]. Although being structurally effective as proved in [TPP+16] and arguably aesthetically charming, so far these grid-shells have struggled to attract architects' interest. We propose a method to fabricate a mockup of the grid shell by using modern additive 3D printing and laser cutting technologies. We also show how the realised mockup can be used to perform a preliminary validation of the simulated static performances of the grid-shell structure.

Categories and Subject Descriptors (according to ACM CCS): I.3.3 [Computer Graphics]: Picture/Image Generation—Line and curve generation

1. Introduction

A lot of effort has been focused in the last years on how architectural structures can be optimised by using geometry processing techniques. Some of these techniques address the optimization of some geometric characteristics to reduce the cost of the fabrication, for example by discretising the set of possible elements composing the final structure. Other techniques aim at improving the static performance of architectural structures to make them safer in critical conditions.

Most of these *architectural geometry* algorithms are usually designed for grid shell structures. Grid-shell structures are a modern response to the ancient need of covering long span spaces. Their supporting structure is made of steel beams connected at joints, while glass covering panels do not contribute to the overall load bearing capacity. The load bearing capacity of a grid-shell is directly related to the connectivity and the shape of its corresponding mesh. Grid-shells, have been used for about over half century in architecture [OR95]. They are compressive structures, i.e. the principal stress comes mainly from axial forces. A robust as well as light grid-shell can be obtained only through a form-finding process [BK01, OKF08] or by optimizing its connectivity [PTP+15, TPP+16].

Many applicative context can take great advantage from a small-scale mockup representing a grid-shell. Architects usually exploits the mockups to judge the impact of the structure on a specific urban context or to simply to have a real feeling of the final structure. Mockup can be used also to performs load tests and judge the overall stability of the real structure.

We propose a practical process to fabricate a mockup of a grid shell that can be used to physically evaluate and assess static and visual characteristic of a digital desing. Our design is cost-effective and easy to fabricate. Most of the pieces composing the structure can be fabricated using laser cutting technique, or by manually but from wooden sticks, with the exception of the joint that have to be individually printed by an additive technique.

We physically built the mockup of a grid shell structure and performed a load test by increasing the external load on some specific point and measured the overall deformation, we found reasonable agreement between numerical and experimental results.

2. Related Work

In *compressive structures*, the principal stress comes mainly from axial forces, and this explains the deep interconnection between them and masonry structures. The performance of a grid shell structure is usually measured by considering its load factor. The collapse load factor is a scalar quantity which represents how many times the load condition can be increased before reaching the structure's collapse: it quantifies the overall *load bearing capacity* of the structure. The maximum displacement norm comes from a linear elastic analysis and gives a measure of the overall *elastic stiffness* of the structure. An ideal grid-shell should have an as high as possible load factor and an as low as possible maximum displacement norm.

The collapse load factor of a grid-shell is directly related to the geometry and the connectivity of its corresponding mesh. As input an initial geometric shape, usually designed by an architect, is taken as a guide to obtain the final structure.

DOI: 10.2312/stag.20161360

The mesh connectivity can be optimized to obtain a good static behavior [PTP+15], e.g., by distributing the load as uniformly as possible among the different beams and by reducing the bending moments in both the beams and the joints. Some comparative parametric analyses [MW13, TPP+16] have been carried out about the influence of the remeshing pattern on the grid-shell load bearing capacity.

2.1. Architectural geometry

Most contributions in this field are concerned with the optimization of geometric properties of polygonal meshes approximating a free-form surface. Many works address the planarity of faces, such the construction of PQ (planar quad) meshes [LPW+06, LXW+11, TSG+14, SB10, YYPM11, ZSW10], CP (circle packing) meshes [SHWP09], and polygonal hex-dominant meshes [CW07, JWWP14, PJH+14, SHWP09, Tro08]. Others try to build meshes from a restricted number of tiles or molds [EKS+10, FLHCO10, SS10, ZCBK12]. A few works address the realization of support structures, parallel meshes and torsion-free meshes [PLW+07, PJH+14, TSG+14]. Among these works, only few focus on the design of a grid topology [CW07, LXW+11, SB10, ZSW10] and just Schiftner and Balzer [SB10] take into account statics.

3. Modelling the Shell

We generated the grid shell structure used to build our model using the approach proposed by [PTP+15]. The idea behind this approach is to perform a static-aware meshing of a given surface that adapts the tessellation to improve static performances.

We get as input a continuos surface modelled as a triangle mesh (see figure 1.a). In the specific test case of the printed mockup the initial shape is the funicular surface that fits the given boundary constraints (four vertices are fixed). The Shell has a side length of 77 meters and it is composed by hollow circular steel beams of 110 mm of diameters and 25 mm of thickness.

We perform a static analysis of the surface using Finite Element Analysis performed using GSA [Oas14]. From this analysis, we obtain an anisotropic, non-Euclidean metric described by a stress tensor. This tensor is composed by two orthogonal directions $\vec{u}$ and $\vec{v}$ which defines the maximum and the minimum stress direction. Intuitively the main idea of [PTP+15] is to change the final tessellation by concentrating faces in the areas with higher stress and elongate the polygonal faces along the maximum stress directions.

Since the maximum and the minimum stress direction are orthogonal, we decouple the scalar and directional information and represent the stress field as a triple $(\vec{u}_n, d, a)$, where $\vec{u}_n$ is a unit-length vector parallel to $\vec{u}$ (see figure 1.b) , $d = ||\vec{u}||$ is the magnitudo of the maximum stress direction (see figure 1.c) and $a = ||\vec{u}||/||\vec{v}||$ is the ratio of the two stress values (see figure 1.d). Hence, the magnitudo of the stress direction define the *density* of the tessellation and the ratio define cells *anisotropy* which are elongated along the direction expressed by $\vec{u}_n$.

In order to obtain the anisotropy and density metric that guide the tessellation, we have to smooth the triple $(\vec{u}_n, d, a)$. This because the data optioned from the Fem analysis can be noisy due to the simulation. The field $\vec{u}_n$ is smoothed as a cross-field, and so the smoothing procedure is invariant on $\pi/2$ rotations in tangent space (see [BZK09]), while the scalar field d and a are smoothed on the domain of the surface. In order to limit the level of anisotropy and density we clamped the values of d and a to 3. In other words, which means that the smaller polygonal face is 3 times smaller than the bigger ones and the maximum, similarly the most elongated face is 3 times longer than larger.

In order to compute the proper meshing according to the input metric, we deform the initial surface, similarly to [PPTSH14]; in this way we transform the anisotropic metric into an Euclidean metric on the deformed surface. We perform Poisson sampling on the deformed surface using [CCS12] in the deformed space and we compute a Centroidal Voronoi Tessellation of sampled points. This diagram is mapped back to the original surface to obtain an Anisotropic Centroidal Voronoi Tessellation (see figure 2).

In order to improve the aesthetics, as well as the planarity of faces of the ACVT, we optimize their shape to make them as similar as possible to stretched regular polygons. To this aim, we adopt a framework which alternate per- polygon and per-vertex fitting steps (see details on [PTP+14]). Another global optimization step is used to make the final tessellation symmetric with respect to the four symmetry planes of the grid shell. An example of anisotropic density varying tessellation of the funicular shell is shown in figure 3.

4. Building the Shell Mockup

Grid shells, just like polygons, are essentially composed of three different elements:

Beams Beams are linear elements that constitute the backbone of the grid shell. Beams are the structural elements of the grid shell and they support the entire weight of the structure. Intuitively, the more the stress is distributed along the direction of the beams the more the structure is robust, because it is absorbed in the compression or extension of the beams.

Joints Beams are interconnected at joints. The shape of a joint is dependent on the number and the direction of the beams that it has to interconnect. However, sometime a joint can be also modelled as modular element that can have enough degrees of freedom to adapt to different connectivities and directions. Obviously, as beams, joints are also structural elements and contribute to support the weight of the grid shell. In order to simplify the analysis joints are usually modelled as infinitely rigid elements during the simulation.

Panels Panels are bidimensional structures that act as a coverage of the grid shell. Usually panels do not act as structural elements, they do to not carry any load except their own weight and eventually some external, uniformly distributed weight, such as snow. As panels are secured on the joints, their carried weight is uniformly distributed over its joints and then released on the underlying beams structure.

Intuitively, if we represent the grid shell as a manifold polygonal mesh, panels correspond to the faces, beams corresponds to edges and joints corresponds to vertices. Finally, another important aspect of a grid shell is its restrain condition: most often grid-shells

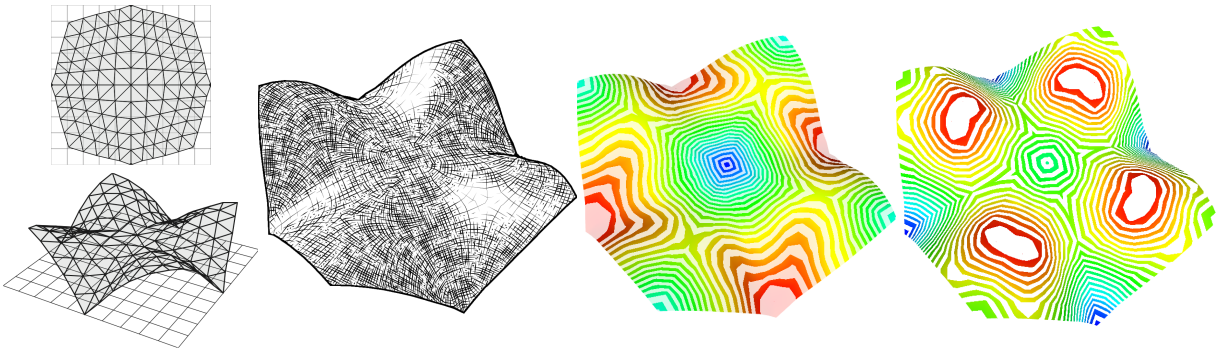

(a) (b) (c) (d)

Figure 1: The initial mesh (a); the stress field direction (b) , the density field (c) and the anisotropy field (d).

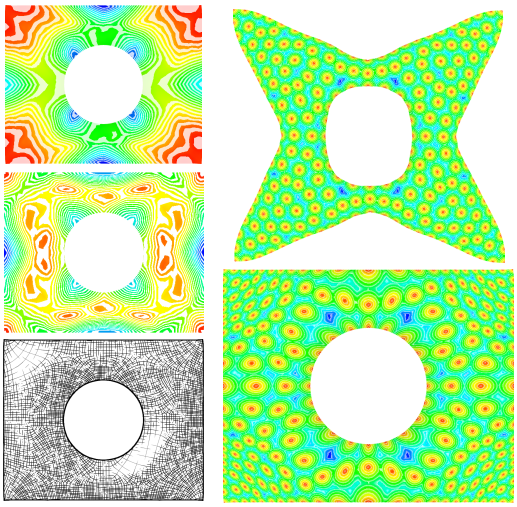

Figure 2: Sampling in deformed space will provide an anisotropic , density varying sampling in undeformed space.

are locally supported on some joints along their boundary. Usually special joints are used to fasten a few beams to the ground, this joints are usually considered as infinitesimally rigid during the Finite element simulation and they are usually modelled as hard constraints.

4.1. Beams

The beams of the mock-up have solid circular cross section with a diameter of 8 mm and an total length of approximately 75 m. Hobby modelling sticks were chosen as building material. A simple script was written in order to univocally number all of the edges as well as to export their cutting length. The 697 beams were then hand-cut, manually labelled and packed in small, manageable bundles. A smaller mockup was also set up in order to double check the viability of the selected construction method, as shown in Figure 4.

4.2. Joints

Joints are modelled to effectively interconnect a set of pipes. Beams are inserted into the joint slots and so kept its correct position. Joints can be generated procedurally given the positions and the cardinality of the adjacent beams. A quick look at Figure 5 reveals that the joints have the same circular cross section of the beams they support. With respect to this Figure: the inner vertical cylinder has a diameter of 24 mm and an height of 10 mm, while the pipes that stem have a 8.25 mm of inner diameter and stick out 21 mm from the inner cylinder.

Joints have been fabricated using an additive 3D printing device. Each joint is located at a vertex of the grid shell and it is aligned along the original surface normal. The upper surface of the joint is carved so as to create a suitable housing for both the three panels converging to the node. Each node has also an hollow where an iron screw and a flat washer are secured to fasten the converging panels.

Because the joints are all different from each other, a number was added along one of the generatrices of the central cylinder to identify them. However, this information was not sufficient to correctly orientate the joint. As the joint size is not big enough to print the beam number on each pipe, a bespoke encoding was devised to conveniently cypher numbers for 3D printing sake. A set of four spheres, coaxial to the beam axis, were introduced. These are let rotate around the axis by multiples of 45 degrees, thus describing a total number of $84 = 2048$ combinations, enough to encompass the 697 beams composing the mock-up. All of the joints were generated in place: in order to 3D print them it was necessary to lay them down onto the horizontal plane, pack them in groups of eight so to fit into the printing tray and export these bundles into .stl format. They have been printed in ABS material by means of an additive 3D printer: each with an average volume of 18 to 20 cm^3 (see Figure 5).

4.3. Panels

As the faces of the grid shell are, in general, not planar, we must account for panels to bend in different directions in order to be placed in their final position. Hence we decided to model

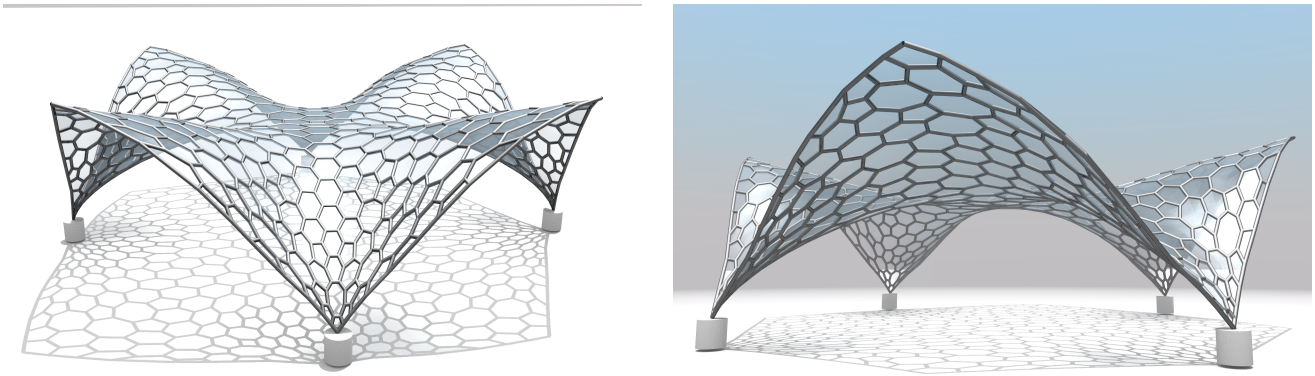

Figure 3: A possible remeshing of the shell surface.

Figure 4: Hand-cut and manually labelled beams, together with a test mock-up.

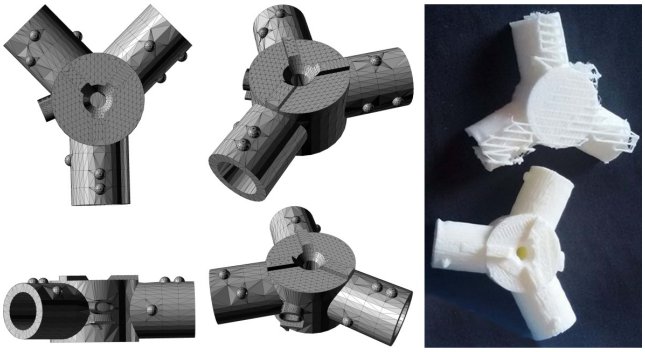

Figure 5: Three dimensional views of joint no. 10 and the printed ones.

the panels using a flexible material. Panels are fabricated with PET sheets, 0.8 mm thick, and cut out using laser cutting technique.

For each polygonal face, we evaluate the best fitting plane and we project its vertices. Hence for each face of the grid shell we obtain a planar polyline that can be packed into the bidimensional rectangular piece of PET ready for the laser-cut machine. Each side of the polylines edges is labelled with the corresponding edge number; these numbers are hetched on the panel using medium laser power. Eventually, all (flat) polylines were packed onto rectangles in order to prepare drawings to be shipped to the laser-cut machine (see figure 6).

As for the joints, a series of scripts was set up in order to generate the planar drawings for the laser-cut machine.

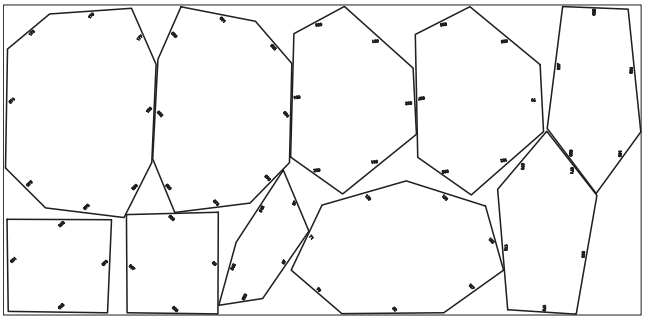

Figure 6: Rectangular sheet filled with planar panels, ready to be laser cut.

4.4. Assembling

A plan view showing the numbering of both beams and joints was essential in order to successfully carry out the delicate assembling procedure. Figure 7 displays a copy of the top view of the grid shell which was used during the construction.

The assembling procedure was rather laborious and it took several days up to completion (figure 8). The structure was built starting from the central part and growing from inside to outside. Temporary scaffolding was used to support the structure until its restraints were put in place. As the structure grew the scaffolding was raised accordingly. The construction sequence was made more difficult by the lack of strength of the 3D printed ABS joints, which kept cracking under the structure self-weight until the four pinned restraints were finally installed.

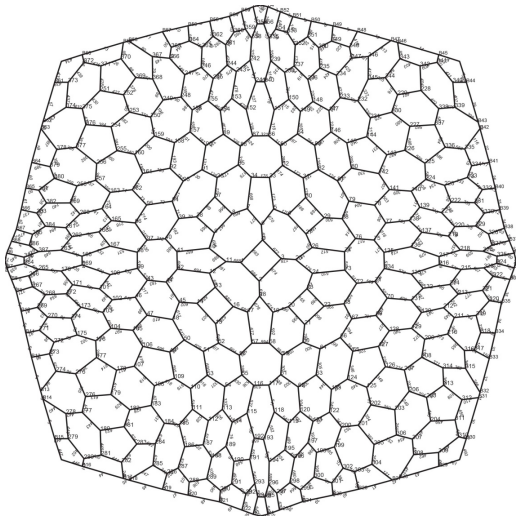

Figure 7: Plan view with the unique numbering of beams and joints used during the construction phase.

Figure 8: Several phases of the construction process.

While panels has been cut from a flat piece of material, the panels of the digital model are not precisely planar. However the such non-planarity is small and it does't effected the overall quality of mockup. The panels are fixed to the joints using some steel washer. The result of the assembly is shown in figure 9. The final mockup is 2.4 meters side length.

Figure 9: The final assembled mockup.

5. Results

We have performed load tests on the physical structure, by incrementally applying weights and monitoring the displacement of the corners of the structure with a proper sensor (see Figure 11.a). The result of the displacement of the vertices with respect to the increment of load is shown in Figure 11.b.

Even if the material of the mockup is considerably different from the one of the simulated real size shell, as shown in Figure 11, there is an excellent agreement between the predicted and the experienced results. The global deformed shape which occurs in correspondence of the buckling of the structure, is nearly the same on both the numerical and the real mode.

6. Conclusions

This work describes a method for the fabrication of a Statics Aware grid-shell mock-up obtained by using the algorithm of [PTP+15]. Particular attention is dedicated to the description of the bespoke procedural approach that was developed in order to carry out this laborious fabrication. As already pointed out in [Fus08], we also believe that nowadays as in the past, design and fabrication are unavoidably affected, steered and often even limited by the availability of suitable tools and software.

As a future work we can include an accurate FEM analysis of on how much the material composing the mockup impacts on the measurement of static properties of the structure. This could help in choosing the right material composing the mockup depending on the test and the material of the final structure.

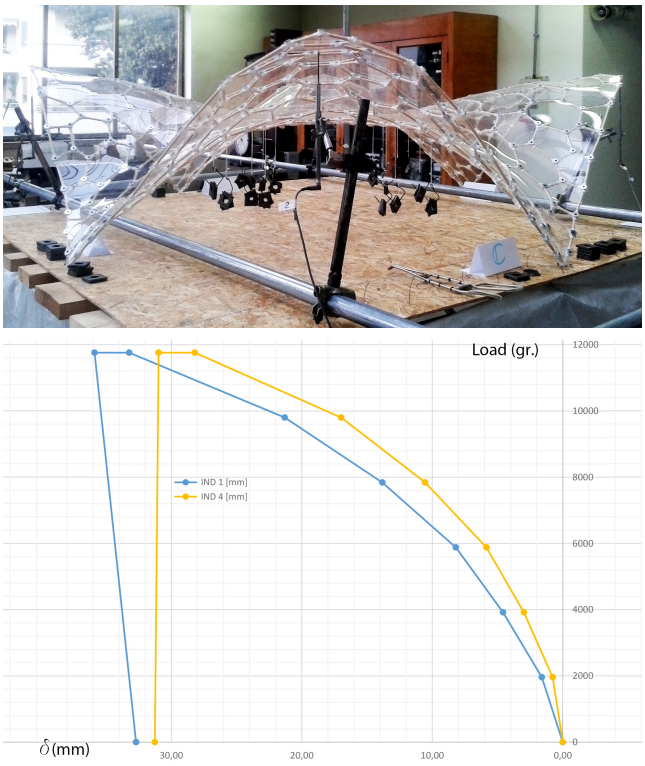

Figure 10: (a) The load test performed on the fabricated mockup; (b) The load/displacement ratio.

To simplify and reduce the needed assembling times we will improve our strategy for generating all the various pieces. For the transparent cover panels we already packed the pieces on separate sheets according to locality criterions. We plan to define a more complete strategy to split the all the pieces of the structure into subportions that can be assembled singularly and connected together to compose the final structure. This advancement could significantly simplify the assembling procedure.

Finally, techniques of topology optimization and joint rationalization can be applied to reduce significantly re production costs.

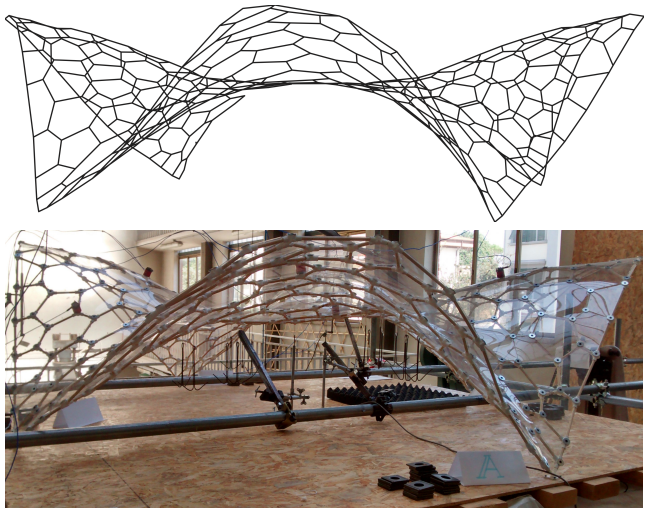

Figure 11: Buckling shape of the mockup: optimal agreement between numerical prediction (Top) and experimental results (Bottom).

References

[BK01] T. Bulenda and J. Knippers. Stability of grid shells. *Computers and Structures*, 79, 2001. 1

[BZK09] David Bommes, Henrik Zimmer, and Leif Kobbelt. Mixed-integer quadrangulation. *ACM Transactions on Graphics*, 28(3):1, July 2009. 2

[CCS12] Massimiliano Corsini, Paolo Cignoni, and Roberto Scopigno. Efficient and flexible sampling with blue noise properties of triangular meshes. *IEEE Transactions on Visualization and Computer Graphics*, 18(6):914–924, 2012. 2

[CW07] Barbara Cutler and Emily Whiting. Constrained planar remeshing for architecture. In *Graphics Interface*, pages 11–18, 2007. 2

[EKS+10] Michael Eigensatz, Martin Kilian, Alexander Schiftner, Niloy J. Mitra, Helmut Pottmann, and Mark Pauly. Paneling architectural freeform surfaces. *ACM Trans. Graph.*, 29(4):45:1–45:10, 2010. 2

[FLHCO10] Chi-Wing Fu, Chi-Fu Lai, Ying He, and Daniel Cohen-Or. K-set tilable surfaces. *ACM Trans. Graph.*, 29(4):44:1–44:6, 2010. 2

[Fus08] Urs Fussler. Design by tools design. *Advances in Architectural Geometry*, 2008. 5

[JWWP14] Caigui Jiang, Jun Wang, Johannes Wallner, and Helmut Pottmann. Freeform honeycomb structures. *Computer Graphics Forum*, 33(5), 2014. Proc. Symp. Geom. Processing. 2

[LPW+06] Yang Liu, Helmut Pottmann, Johannes Wallner, Yong-Liang Yang, and Wenping Wang. Geometric modeling with conical meshes and developable surfaces. *ACM Trans. Graph.*, 25(3):681–689, 2006. 2

[LXW+11] Yang Liu, Weiwei Xu, Jun Wang, Lifeng Zhu, Baining Guo, Falai Chen, and Guoping Wang. General planar quadrilateral mesh design using conjugate direction field. *ACM Trans. Graph.*, 30(6):140:1–140:10, 2011. 2

[MW13] Samar Malek and Chris Williams. Structural implications of using cairo tiling and hexagons in gridshells. In *Proceedings of the International Association for Shell and Spatial Structures (IASS) Symposium 2013*, 2013. 2

[Oas14] Oasys. Gsa analysis, 2014. http://http://www.oasys-software.com. 2

[OKF08] Toshiyuki Ogawa, Shiro Kato, and Masumi Fujimoto. Buckling load of elliptic and hyperbolic paraboloidal steel single-layer reticulated shells of rectangular plan. *Journal of the International Association for Shell and Spatial Structures*, 2008. 1

[OR95] F. Otto and B. Rash. *Finding Form*. Edition Alex Menges, Stuttgart, 1995. 1

[PJH+14] Helmut Pottmann, Caigui Jiang, Mathias Höbinger, Jun Wang, Philippe Bompas, and Johannes Wallner. Cell packing structures. *Computer-Aided Design*, pages 1–14, March 2014. 2

[PLW+07] Helmut Pottmann, Yang Liu, Johannes Wallner, Alexander Bobenko, and Wenping Wang. Geometry of multi-layer freeform structures for architecture. *ACM Trans. Graphics*, 26(3), 2007. 2

[PPTSH14] Daniele Panozzo, Enrico Puppo, Marco Tarini, and Olga Sorkine-Hornung. Frame fields: Anisotropic and non-orthogonal cross fields. *ACM Trans. Graph.*, 2014. to appear. 2

[PTP+14] Nico Pietroni, Davide Tonelli, Enrico Puppo, Maurizio Froli,

Roberto Scopigno, and Paolo Cignoni. Voronoi grid-shell structures. *CoRR*, abs/1408.6591, 2014. 2

[PTP+15] Nico Pietroni, Davide Tonelli, Enrico Puppo, Maurizio Froli, Roberto Scopigno, and Paolo Cignoni. Statics aware grid shells. *Computer Graphics Forum (Special issue of EUROGRAPHICS 2015)*, 34(2):627–641, 2015. 1, 2, 5

[SB10] Alexander Schiftner and Jonathan Balzer. Statics-sensitive layout of planar quadrilateral meshes. In Cristiano Ceccato, Lars Hesselgren, Mark Pauly, Helmut Pottmann, and Johannes Wallner, editors, *Advances in Architectural Geometry 2010*, pages 221–236. Springer Vienna, 2010. 2

[SHWP09] Alexander Schiftner, Mathias Höbinger, Johannes Wallner, and Helmut Pottmann. Packing circles and spheres on surfaces. *ACM Trans. Graph.*, 28(5):139:1–139:8, 2009. 2

[SS10] Mayank Singh and Scott Schaefer. Triangle surfaces with discrete equivalence classes. *ACM Trans. Graph.*, 29(4):46:1–46:7, 2010. 2

[TPP+16] Davide Tonelli, Nico Pietroni, Enrico Puppo, Maurizio Froli, Paolo Cignoni, Gennaro Amendola, and Roberto Scopigno. Stability of statics aware voronoi grid-shells. *Engineering Structures*, 116(1):70–82, june 2016. original paper at http://www.sciencedirect.com/science/article/pii/S0141029616300074. 1, 2

[Tro08] Christian Troche. Planar hexagonal meshes by tangent plane intersection. *Advances in Architectural Geometry*, 1:57–60, 2008. 2

[TSG+14] Chengcheng Tang, Xiang Sun, Alexandra Gomes, Johannes Wallner, and Helmut Pottmann. Form-finding with polyhedral meshes made simple. *ACM Trans. Graph.*, 2014. to appear. 2

[YYPM11] Yong-Liang Yang, Yi-Jun Yang, Helmut Pottmann, and Niloy J. Mitra. Shape space exploration of constrained meshes. *ACM Trans. Graph.*, 30(6):124:1–124:12, 2011. 2

[ZCBK12] Henrik Zimmer, Marcel Campen, David Bommes, and Leif Kobbelt. Rationalization of triangle-based point-folding structures. *Comp. Graph. Forum*, 31(2pt3):611–620, 2012. 2

[ZSW10] Mirko Zadravec, Alexander Schiftner, and Johannes Wallner. Designing quad-dominant meshes with planar faces. *Computer Graphics Forum*, 29(5):1671–1679, 2010. Proc. Symp. Geometry Processing. 2